applied sciences

MDPI

Article

The Safe Passage Redundancy Analysis of Airport Taxiway Bridge Based on Aircraft Load Fatigue Accumulation

Yuhui Zhang and Yuanyuan Zhao *

College of Transportation Science and Engineering, Civil Aviation University of China, Tianjin 300300, China
* Correspondence: yuanyuan_zhao2022@163.com

Abstract: This paper is centered around the theoretical, experimental, and simulation analysis of safe passage redundancy and the mechanical deformation of the taxiway bridge under the fatigue accumulation state, and we define the redundancy as the remaining times that the aircraft can pass safely on the taxiway bridge. Based on the principle of stress control, the entity of the taxiway bridge was scaled to establish a laboratory model. The accuracy of the simulation model was verified by the comparative analysis between the experimental and the simulation data. The fatigue–life curve (S–N curve) was introduced to overlay the material fatigue state cycle into the simulation model of the taxiway bridge, and the safe passage redundancy and mechanical deformation of the bridge under the fatigue accumulation state were analyzed. By analyzing and processing the simulation data, a calculation model for the safe passage degree of the taxiway bridge under the fatigue state and a prediction calculation model for the remaining passage life were constructed. By comparing the simulation data with the model data, the accuracy of the established model was verified to be higher than 95%, which provides an important theoretical reference for the development of research on the safety life detection and evaluation of the subsequent taxiway bridge under the fatigue state.

Keywords: taxiway bridge; safe passage redundancy; mechanical deformation; fatigue cumulative; life prediction of taxiway bridge

Citation: Zhang, Y.; Zhao, Y. The Safe Passage Redundancy Analysis of Airport Taxiway Bridge Based on Aircraft Load Fatigue Accumulation. *Appl. Sci.* **2023**, *13*, 1164. https://doi.org/10.3390/app13021164

Academic Editors: Hernâni Miguel Reis Lopes and Elza Maria Morais Fonseca

Received: 21 December 2022
Revised: 11 January 2023
Accepted: 12 January 2023
Published: 15 January 2023

1. Introduction

With the development of the civil aviation industry, airport throughput increases year by year, and many new aircraft types are utilized. As an important facility used to solve the conflict between aircraft ground taxiing and vehicle driving routes in the flight area, airport taxiway bridges as shown in Figure 1 is critical for the safety of the flight area and the efficient operation of aircraft. Different from the continuous tiled vehicle load of traditional bridges, the load on the bridge deck of the taxiway bridge is the moving load of the aircraft, while the vehicles pass under the bridge. This special load mode brings great difficulties in later maintenance and detection. Generally speaking, the design service life of the taxiway bridge is 20 years. In actual operation, it is often used for more than 10 years without any detection. The safe capacity under the fatigue state is unknown, and there are various security risks such as wall cracking, concrete spalling, and steel bar exposure. Because on-site inspection needs to interrupt traffic and long-term loading test conditions, and the particularity of aircraft moving load will lead to local loads more than six times higher than the vehicle loads of conventional bridges, the detection experience of traditional ports and highway bridges is not applicable. Furthermore, the particularity of the design of the taxiway bridge leads to its cross runway, and the site construction and detection will have a great impact on the operation of the whole airport. At present, there is relatively little research on this special bridge in the world. Researchers have focused on establishing and optimizing the simulation modeling of the taxiway bridge [1–5] and the mechanical property test [6–8]. In the field of traditional bridges, there are many studies on fatigue performance. Through various methods such as the

simulation model [9–15] and experimental research [16–21], the fatigue change mechanism and mechanical deformation of traditional bridges under vehicle load has been revealed, and the fatigue damage prediction model and the life prediction model have been deduced. However, as mentioned above, due to the great differences between the taxiway bridge and the traditional bridge in the bridge structure, aspect ratio, pavement material, roughness, and texture depth, there is no evaluation standard for its safe passage.

Figure 1. Taxiway bridge entity image.

By way of considering the above problems, finite element software is used to model the entity of the taxiway bridge, and the simulation data are fitted. The model used to calculate the fatigue safety passage redundancy of the taxiway bridge is deduced, and then the formula is used to predict the safe passage redundancy of the taxiway bridge. This formula can effectively break through these limitations, thus making it an effective method.

2. Emulation Modeling

2.1. Engineering Background

Simulation modeling analysis is carried out on an airport taxiway bridge entity in South China. The airfield area class of this airport is 4 E. The taxiway bridge has a length of 44 m and a width of 65.5 m. The bridge is composed of two spans with a simply supported beam bridge; each span has a length of 15.62 m, a width of 65.50 m, and a height of 1.30 m. The bridge deck is a multi-cell box girder, and the box body is a variable section octahedron. The main beam is C50 concrete, and the abutment is C30 concrete. Rubber bearing is laminated rubber bearing, which mainly bears the vertical load and has a large vertical stiffness. It is made of multilayer rubber and steel plate. The taxiway bridge takes the representative aircraft Boeing 747-400 of the E-type civil aviation airport as the design calculation load and Boeing 777-300 and MD-11 as the checking load.

2.2. Method of Applying Aircraft Load

The interaction range between the aircraft and the pavement is a contact surface. Due to the small area of the contact surface relative to the pavement area, the stress distribution in the middle and the edge of the wheel tends to be uniform. At the same time, to improve the operation efficiency of the model, the moving load of the aircraft can be simplified as a loaded treatment applied according to the wheel print area. According to pavement design specification [22,23], the shape is composed of the semicircle and the rectangle, as shown in Figure 2.

The wheel seal width (W_t) of the main landing gear of the aircraft is 0.6 times the wheel seal length (L_t), and the wheel seal length is determined according to the Equation (1):

$$L_t = \sqrt{\frac{P \times 10^4}{5.227q}} \tag{1}$$

The units of the wheel print length and width in millimeters are shown. q (MPa) is the tire pressure of the main landing gear and P (kN) is the single-wheel load value of the aircraft's main landing gear.

In the finite element software, after the aircraft wheel print is applied to the pavement, the contact between the wheel print and the bridge deck is set as the contact between the surface and the surface, the contact attribute is set as tangential and normal, and the applied downward pressure is set to the wheel print. Finally, the implicit dynamic solution analysis step is adopted, and the incremental step type is fixed to realize the application of the aircraft moving load.

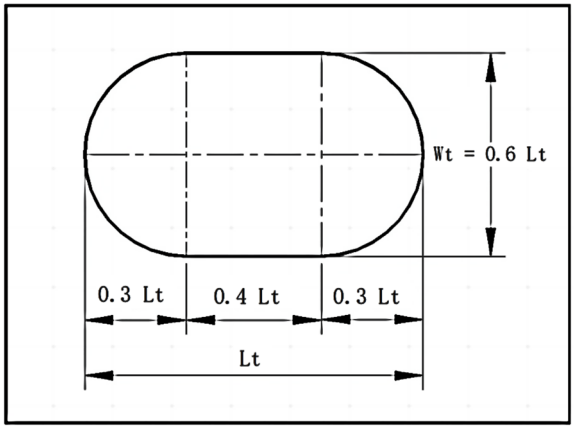

Figure 2. Schematic diagram of wheel print shape.

2.3. Construction of the Taxiway Bridge Simulation Model

The deck of the taxiway bridge is a prestressed reinforced concrete composite structure. Thus, the separate modeling method is adopted. The prestressed steel strand has a strength of Φ15; the low relaxation steel strand is arranged in two rows of upward bending reinforcement, and the reinforcement in the same row is the same. The bending angle of the upper row of reinforcement is 7.1°, and the bending angle of the lower row of reinforcement is 4.3°, with four bars for each cluster (32 clusters in total). The design standard strength is 1860 MPa, and the control tensile stress is 1395 MPa.

During modeling, the cooling method is used to simulate the prestressed reinforcement. When the temperature decreases, the prestressed reinforcement shrinks, and the strain is transferred from the shrinkage between the prestressed reinforcement and the concrete to other parts. The calculation equation is as follows:

$$\Delta T = \frac{\delta}{E_s \alpha} \tag{2}$$

In Equation (2), ΔT represents the size of cooling; δ represents the applied prestress value (MPa), which is 1395 MPa; Es is the elastic modulus of reinforcement (MPa); and α is the coefficient of thermal expansion, which is 1.2×10^{-5}.

The reinforcement grid and concrete are coupled via a built-in connection. The "embedding" function is used to embed the reinforcement into the concrete to simulate the actual position of the reinforcement grid in the concrete, as well as to establish the coupling relationship between the reinforcement and concrete.

Piers and abutments are not components directly bearing aircraft load, and their internal reinforcement is evenly distributed. To improve the calculation efficiency of the finite element model (FEM), the reinforcement is dispersed into the concrete for integral modeling purposes.

The "spring damper" function is used to simulate the plate rubber bearing. According to the specification of the Ministry of Communications of the People's Republic of China

(JT/T4-2004), the compressive elastic modulus of the bearing is calculated according to the Equation (3):

$$E = 5.4\,GS^2 \tag{3}$$

E (MPa) is the compressive elastic modulus of the bearing. G (MPa) is the shear elastic modulus of bearing, which is 1.5 MPa. S is the bearing shape factor, which is 0.86.

According to the Equation (3), the plate rubber bearing is simplified equivalently: the contact surface between the rubber bearing and the substructure is cut, the position of the bearing center point is determined, and the spring damper function is used to add a spring component between the corresponding points. The spring is linearly elastic. The elastic modulus of the rubber bearing is 6 MPa, and the spring stiffness is set to 2.03 [24].

The taxiway bridge studied in this paper is located in South China and belongs to the soft soil foundation area [25]. After consulting the local geological survey report, it can be seen that the foundation's elastic modulus is 19.86 MPa. The Winkler foundation model is selected to set the soil spring at the bottom of the bridge for foundation simulation. The elastic modulus of soil spring is set based on the elastic modulus of soil foundation. The side walls on both sides of the bridge and the partition wall in the middle impose freedom constraints in the x and y directions. Hexahedral elements are used to mesh the model. The overall model and grid division of the taxiway bridge are shown in Figure 3.

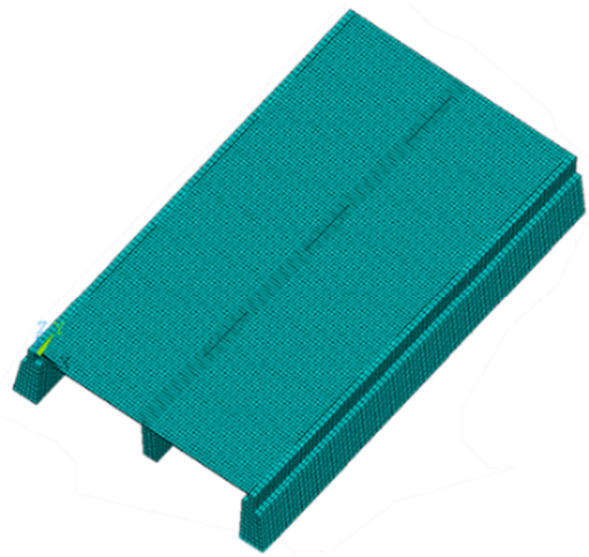

Figure 3. FEM of the taxiway bridge.

2.4. Finite Element Model Accuracy Verification

Under the action of the aircraft moving load, the stress distribution of each section of the taxiway bridge deck shows a certain trend [26]. After on-site inspection, the stress of key nodes was reduced in the same proportion, and on this basis, the bridge deck laboratory model conforming to the reduced stress distribution was poured. The size of the laboratory bridge deck model was 7.5 cm × 30 cm × 13 cm. The measured data in the laboratory were compared with the simulation data, and the FEM was adjusted to improve the accuracy of the finite element model and verify the identity and accuracy of the theoretical deduction and simulation model.

To verify the accuracy of the model, B747-400, with a load of 2643.55 kN, was used to conduct a field loading test on the taxiway bridge. The west support, the middle support of the first span, the middle support, the middle support of the second span, and the East support of the centerline of the taxiway bridge deck are numbered as 1, 2, 3, 4, and 5, respectively. The longitudinal section layout of the bridge is shown in Figure 4.

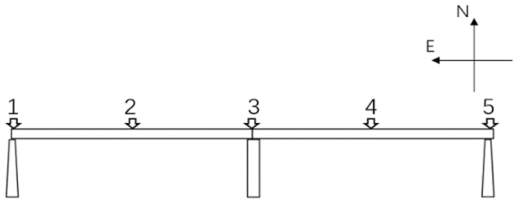

Figure 4. Longitudinal section layout of the bridge.

Strain sensors and inclination sensors were installed along the centerline of the bridge deck to record the measured deflection, stress, and strain values of key nodes, and the operation results of the simulation model were then compared, as shown in Table 1. The simulated deformation cloud chart of the bridge under the load at point 1 is shown in Figure 5.

Table 1. FEM accuracy verification table.

Point Number	Deflection Value (mm)			Stress Value/kN			Strain Value/$\times 10^{-3}$		
	Measured Value	Simulation Value	Relative Error	Measured Value	Simulation Value	Relative Error	Measured Value	Simulation Value	Relative Error
1	−3.46	−3.60	4.14%	−1652.33	−1713.80	3.72%	1.28	1.34	4.74%
2	−7.89	−8.20	3.95%	−1427.54	−1486.78	4.15%	1.93	2.00	4.03%
3	−1.07	−1.12	4.86%	−1732.61	−1803.30	4.08%	0.82	0.86	4.85%
4	−8.18	−8.51	4.03%	−1396.80	−1451.70	3.93%	2.17	2.24	3.26%
5	−3.70	−3.86	4.23%	−1603.79	−1675.16	4.45%	1.46	1.52	4.31%

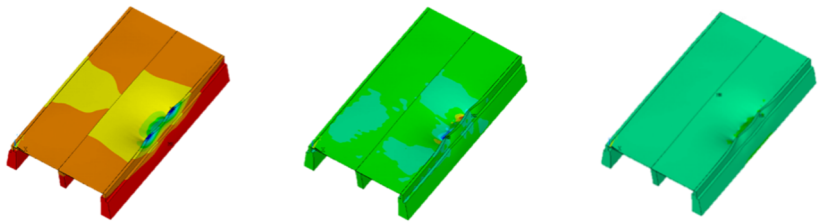

(**a**) (**b**) (**c**)

Figure 5. Cloud chart of bridge deformation loadings at point 1: (**a**) cloud chart of deflection; (**b**) cloud chart of strain; (**c**) cloud chart of stress.

The table shows that the simulation data are highly consistent with the measured data in many indexes, and the relative error value can be controlled below 5%, which is greater than the field measured value. Under this condition, the simulation results can be guaranteed to be accurate and reliable.

3. Theoretical Analysis

3.1. Normalization of the Aircraft Load

Based on the actual data statistics of an airport taxiway bridge in South China, many types of aircraft run on the airport taxiway bridge, and different types of aircraft have different effects on the deformation and fatigue accumulation of the taxiway bridge. Therefore, the aircrafts passing on the taxiway bridge are normalized and converted to B747-400. According to the "Code for design of cement concrete pavement of civil airport", the proposed aircraft load conversion model is shown in Equation (4) [27,28]:

$$P_t = \frac{Gp}{n_c n_w} \tag{4}$$

P_t is the wheel load on the main landing gear of the aircraft (kN), G is the aircraft weight (kN), p is the load distribution coefficient of the main landing gear, n_c is the number of main landing gears, and n_w is the number of wheels on one main landing gear.

We define the single-wheel load conversion factor K_t of aircraft below to convert the wheel load of other aircraft types into the wheel load of standard types:

$$K_t = \frac{P_{tn}}{P_{t0}} \tag{5}$$

P_{tn} (kN) is the single-wheel load value of the type to be converted under a certain load state and P_{t0} (kN) is the single-wheel load value of the standard aircraft type under the same load state.

The final conversion results of various aircraft loads under different load states are shown in Table 2.

Table 2. The single-wheel load conversion of different aircraft types.

Aircraft Type	Aircraft Weight in Different Conditions/kN		Load Distribution Coefficient of the Main Landing Gear	Number of Main Landing Gears	Number of Wheels on One Main Landing Gear	Single-Wheel Load of Main Landing Gear/kN	Conversion Factor Kt
B737-300	Basic weight	326.02	0.950	2	2	77.43	0.71
	Maximum landing weight	517.09				122.81	0.72
	Maximum ramp weight	566.99				134.66	0.57
B737-800	Basic weight	414.30	0.950	2	2	98.40	0.91
	Maximum landing weight	663.80				157.65	0.93
	Maximum ramp weight	792.60				188.24	0.80
A320-200	Basic weight	405.29	0.950	2	4	48.13	0.44
	Maximum landing weight	645.00				76.59	0.45
	Maximum ramp weight	774.00				91.91	0.39
B777-300	Basic weight	1578.00	0.948	2	6	124.66	1.15
	Maximum landing weight	2376.80				187.77	1.10
	Maximum ramp weight	3002.80				237.22	1.00
B747-400	Basic weight	1827.21	0.952	4	4	108.72	/
	Maximum landing weight	2857.63				170.03	/
	Maximum ramp weight	3978.00				236.69	/

3.2. The Fatigue Equivalent of the Taxiway Bridge Based on the S–N Curve

The stress–life curve (S–N curve) takes the fatigue strength of the material standard specimen as the ordinate and the logarithm lgN of the fatigue life as the abscissa to represent the relationship between the fatigue strength and the fatigue life of the standard specimen under the characteristic cycle characteristics. The S–N curve can reflect the relationship between the fatigue strength and the fatigue life. When studying the fatigue strength of the structure, the S–N curve of its constituent materials plays an important role in the operation cycle, fatigue characteristics, and applicable redundancy of the whole structure [21].

For the superstructure of the studied taxiway bridge, the fatigue of the bridge deck is mainly reflected in the fatigue of the reinforcement and concrete. The repeated aircraft load changes the structural and material parameters of the taxiway bridge, resulting in a reduction in the bearing capacity and the maximum deflection exceeding the specification requirements.

According to the design drawings, the main beam in the superstructure of the taxiway bridge adopts C50 concrete, and the prestressed steel strand is Φ15 high strength low relaxation steel strand. Through on-site core drilling sampling, compression, splitting, and fatigue tests are carried out. By querying the existing research and specifications [29–32], the results of hundreds of load tests in the laboratory are compared with the results in the existing literature and specifications. It is found that they are consistent. Therefore, the fatigue parameter values and S–N curves obtained by referring to the existing research and specifications are shown in Table 3.

Table 3. The fatigue test values of the reinforcement and concrete.

Number of Cycles	Yield Stress of Reinforcement/MPa	Compressive Stress of Concrete/MPa	Concrete Tensile Stress/MPa
1585	485	25.30	1.89
2512	470	24.52	1.83
3981	455	23.74	1.77
6310	440	22.95	1.71
10,000	425	22.17	1.66
15,849	410	21.39	1.60
25,119	395	20.61	1.54
39,811	380	19.82	1.48
63,096	365	19.04	1.42
100,000	350	18.26	1.36
158,489	335	17.48	1.31
251,189	320	16.69	1.25
398,107	305	15.91	1.19
630,957	290	15.13	1.13
1,000,000	275	14.35	1.07
1,585,000	260	13.56	1.01
2,512,000	245	12.78	0.95
3,981,000	230	12.00	0.90
6,310,000	215	11.22	0.84
10,000,000	200	10.43	0.78

As shown in Figure 6, the abscissa cycle times represent the times of repeated application of aircraft load, and the ordinate represents the yield stress of the reinforcement under the application of the repeated aircraft load, the tensile stress of concrete on the lower surface of the bridge deck, and the compressive stress of concrete on the upper surface of bridge deck along the action line of aircraft. From the three stress–life curves, it can be seen that the material strength of the concrete and reinforcement sharply decreases in the first 1 million cycles, and the decline rate greatly slows down in the process of the first 1 million to 10 million cycles, thus providing an effective idea for the application of subsequent loads and the study of the fatigue characteristics of the taxiway bridge during fatigue analysis. Firstly, the aircraft sorties passing through the bridge deck in a year are counted, and then the annual sorties are converted into operation times, corresponding to the S–N curves of the reinforcement and concrete materials to obtain the fatigue strength parameters of the two materials, which are then inputted into the simulation software for operation purposes to obtain various strength check indexes of the taxiway bridge under the fatigue state, such as maximum deflection, stress value, strain value, etc. Moreover, checks are made to determine whether the fatigue strength of the bridge meets the operation requirements of the current model.

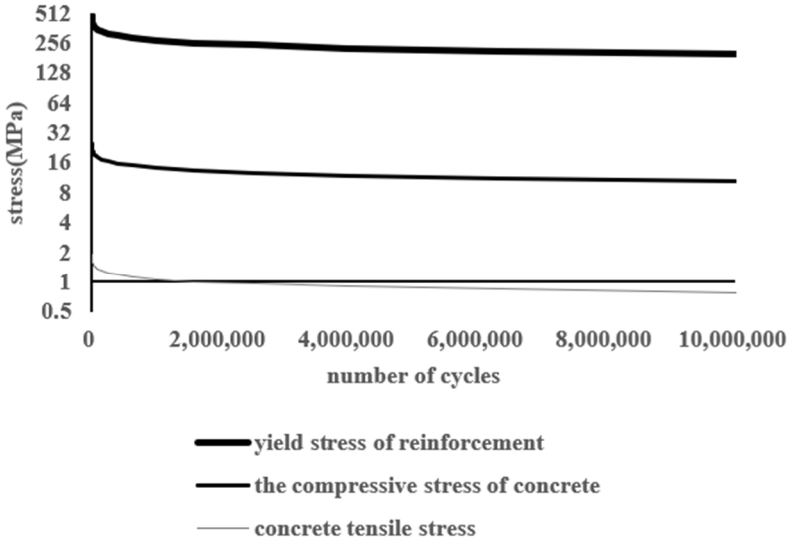

Figure 6. The S–N curve of reinforcement and concrete.

3.3. Establishment of the Safe Passage Redundancy Index of the Taxiway Bridge

The passage redundancy of the taxiway bridge is also studied under the fatigue accumulation state. Safe passage redundancy refers to the remaining times that the aircraft can safely pass through the taxiway bridge.

Currently, the most widely used strength verification method in the field of bridge fatigue strength is the verification of the maximum deflection in the middle of the span. This verification method has the advantages of obvious change, strong regularity, and can be detected without on-site loading. Therefore, this method is used to quantitatively analyze the fatigue safety passage redundancy of the taxiway bridge.

Article 4.2.3, titled "Code for the design of highway reinforced concrete and prestressed concrete bridges and culverts" (JTJ023-85), provides the design specifications for taxiway bridges, and points out that the maximum deflection of the upper bearing structure of the bridge with a reinforced concrete structure calculated by the operating load (excluding the impact force) shall not exceed the following values.

In Table 4, L is the calculated span (mm) and L_1 is the cantilever length (mm).

Table 4. The allowable maximum deflection of each part of the bridge.

Position	Allowable Maximum Deflection
The mid-span of the girder of the beam bridge	$1/600\ L$
The cantilever end of the girder of the beam bridge	$1/300\ L_1$
The truss, arch	$1/800\ L$

According to the design drawing of the taxiway bridge, the bridge deck is composed of two spans simply supported beams, and the maximum deflection value of the bridge deck appears at the mid-span of each span. Therefore, it can be seen that the allowable maximum deflection value is $1/600\ L$ = 26.03 mm, meaning that when the aircraft passes the taxiway bridge for the Nth time, if the maximum deflection value is generated by the action line between the wheel and the bridge deck at the mid-span (hereinafter referred to as the maximum deflection value at the mid-span) is greater than 26.03 mm, the bridge meets the fatigue end standard and no longer meets the needs of safe passage.

According to statistics, the taxiway bridge studied in this study sees 35 aircraft every day on average. If the flight growth rate is not considered, the cumulative traffic sorties in the whole life cycle (20 years) can be calculated from this. Referring to the standard aircraft type of taxiway bridge operation of the airport, B747-400 is selected as the standard aircraft type, and the takeoff and landing structure type and load value (2857.63 kN are inputted

into the FEM to obtain the mid-span deflection values of the two spans of the taxiway bridge. Since the mid-span deflection values of the two spans of the taxiway bridge has little difference, the maximum mid-span deflection value of the two spans is selected as the maximum mid-span deflection value. The relationship between the maximum deflection value in the span and the number of aircraft operations is shown in Table 5.

Table 5. The relationship between the taxiway bridge deflection and aircraft operation times.

Aircraft Operation Times *N*	Maximum Deflection Value in the Mid-Span/mm	Allowable Maximum Deflection/mm
0	1.3715	26.03
12,775	3.41	
63,875	6.87	
127,750	10.36	
191,625	17.38	
255,500	24.49	

It can be observed from the table that with the increase in operation times, the maximum deflection value in the middle of the span increases, but it is less than the allowable maximum deflection value in the whole life cycle, and the absolute value of the difference between the two is 1.54 mm, indicating that the fatigue performance of the taxiway bridge still meets the requirements of safe passage after 255,500 sorties of the standard model under this loading state [33].

To sum up, if the functional relationship between the mid-span deflection value and operation times can be deduced, combined with the conversion formula between the loads of different models shown in Section 3.1, the safe passage redundancy of the taxiway bridge can be effectively predicted after the combined model load is operated for several times, and its fatigue performance can be quantitatively analyzed.

4. Construction of the Safety Passage Redundancy Evaluation Model for the Taxiway Bridge

4.1. Quantitative Analysis of the Relationship between the Fatigue State and the Safe Passage Redundancy of the Taxiway Bridge

Based on the analysis shown in Section III, the changing trend of the maximum deflection value in the middle of the two spans of the taxiway bridge can be used to analyze the fatigue characteristics of the taxiway bridge. Exceeding the allowable maximum deflection value in the middle of the bridge indicates that the bridge reaches the fatigue end standard. The maximum deflection value in the middle of the taxiway bridge is selected as the key index of the safe passage redundancy of the taxiway bridge and B747-400 is selected as the standard aircraft type. The number of aircraft and the aircraft load in relation to the taxiway bridge deck both play a key role in the fatigue accumulation of the taxiway bridge. This chapter intends to establish the change relationship model between the operation times, the operation load, and the maximum deflection in the middle of the span of the aircraft on the taxiway bridge in order to construct the quantitative relationship between the fatigue state and safe passage redundancy.

By taking the maximum landing weight (2857.63 kN) of the standard aircraft type B747-400 as the operation load, according to the 35 flights per day of the taxiway bridge, about 255,500 operation sorties of the taxiway bridge are calculated within the specified design life of 20 years. Therefore, 0–255,500 is used as the operation time value to operate on the established FEM of the taxiway bridge.

The maximum deflection value in the middle of the span of 0–255,500 operations is derived, and the correlation between the maximum deflection value in the middle of the span and the operation times is analyzed [34]. The relationship is as follows:

$$Y = 10^{-10}N_t{}^2 + 7 \times 10^{-5}N_t + Y_c \quad (6)$$

Y (mm) is the maximum deflection value of the bridge deck mid-span; N_t is the total number of aircraft sorties that can operate under the existing load state; and Y_c (mm) is the mid-span deflection caused by the weight of the taxiway bridge. The initial state of the taxiway bridge (load = 0, operation time = 0) is inputted into the finite element simulation software. The maximum deflection value in the middle of the span is 1.3715 mm, indicating that the deflection value caused by its own weight is 1.3715 mm. The curve is shown in Figure 7, with the dotted line representing the fitting curve:

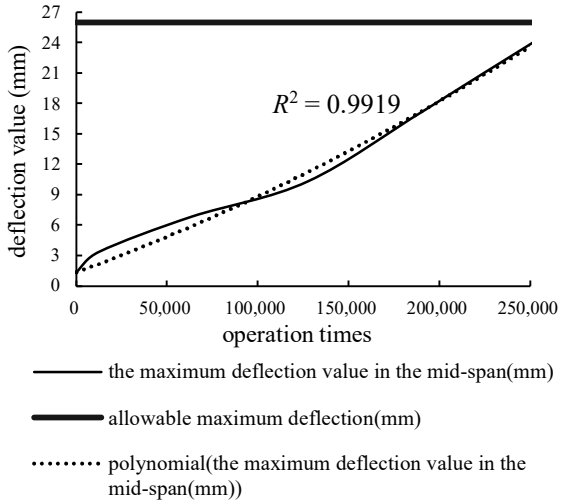

Figure 7. The relationship between taxiway bridge deflection and aircraft operation times.

According to various calculations, the correlation coefficient $R^2 = 0.9919$, indicating that the correlation degree of this curve to the data is as high as 99.19%, is very much in line with the prediction requirements [28].

Therefore, it can be concluded that the safe passage redundancy of the taxiway bridge under a standard aircraft load type is:

$$N_s = N_t - N_0 \tag{7}$$

N_s is the safe passage (sorties) and N_0 is the sorties that are now operated.

According to the fatigue formula inferred from the above data, by substituting the allowable maximum deflection value of the bridge deck into 26.03 mm, it can be obtained that the difference between the maximum deflection value and the allowable maximum deflection value of the taxiway bridge under this fatigue state is 0.25 mm, and 2023 sorties B747-400 can still pass safely with the maximum landing weight [35]. Due to the small difference between 255,500 and 257,023, in the subsequent calculation, 255,500 can be taken as the maximum number of passes of the standard aircraft type under the maximum landing weight.

To verify the reliability of the above formula, the operation times to 300,000 sorties extract the data every 4450 sorties, and the deduced value of the relationship can be compared with the simulation output value of the FEM. Thus, the following curve can be obtained as shown in Figure 8:

The above verification data show that the formula deduced for the taxiway bridge in this operating state is accurate, the trend of the calculated value is consistent with the simulation value, and the relative error is controlled within 5%, thus demonstrating its reliability.

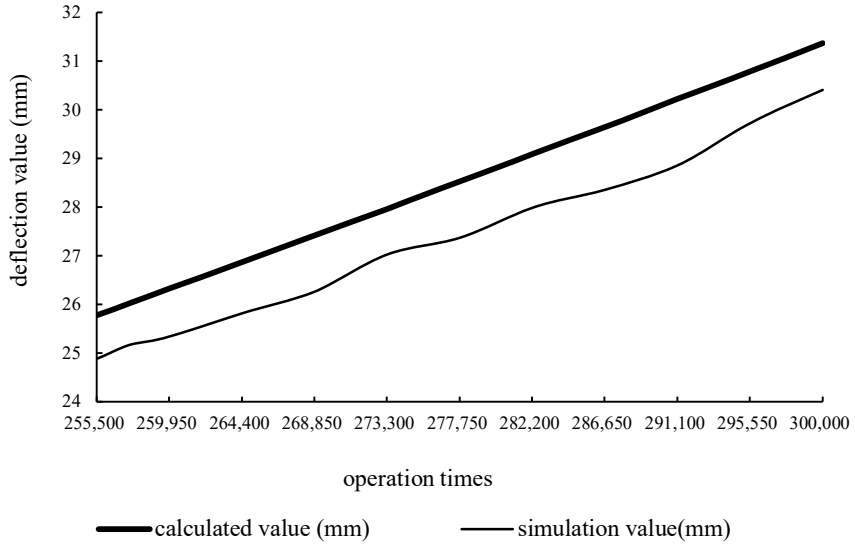

Figure 8. Data validation curve.

4.2. Analysis of the Maximum Allowable Load of the Taxiway Bridge Based on the Maximum Number of Passes

According to the analysis in the previous section, the taxiway bridge can operate at least 255,500 times in association with the maximum landing weight in the specified life cycle. Considering the difference between the basic weight of the aircraft and the full weight of the aircraft, as well as the influence of the aircraft seating rate and other factors on the size of aircraft load, it is therefore necessary to explore the relationship between different load sizes of standard aircraft type B747-400 and the maximum deflection value in the middle span of the taxiway bridge under the maximum operation times to make the load reduction measures appropriate for the safe operation of the taxiway bridge.

The standard aircraft type B747-400 operates 255,500 times in the FEM with a basic weight of 1827.21 kN, a maximum landing weight of 2857.63 kN, a maximum take-off weight of 3968.93 kN, and a maximum ramp weight of 3978.00 kN. The data of the maximum deflection value in the middle of the span after operation are derived, and the correlation between the maximum deflection value in the middle of the span and the load is analyzed. The relationship between the maximum deflection value in the span and the load is obtained as follows:

$$Y = 0.0079Q_t + Y_c \quad (8)$$

Y (mm) is the maximum deflection value of the bridge deck mid-span; Q_t (kN) is a load of the standard aircraft type; Y_c (mm) is the mid-span deflection caused by the weight of the taxiway bridge. The curve is shown in Figure 9, and the dotted line represents the fitting curve.

With the increase in load, the maximum deflection at the mid-span increases linearly, and the correlation coefficient $R^2 = 0.9864$, indicating that the correlation degree of the curve to the data is as high as 98.64%. According to this relationship, the allowable maximum deflection value $Y = 26.03$ mm, the load $Q_t = 3121.33$ kN can be obtained, indicating that the standard aircraft type needs a load reduction, and the maximum can only operate 255,500 times with the load value of 3121.33 kN to ensure the safe passage of the aircraft.

For the above relationship, the following curve can be obtained as shown in Figure 10 by increasing the aircraft load value to 4500 kN without considering the limitations of the code and taking ten verification nodes for verification purposes.

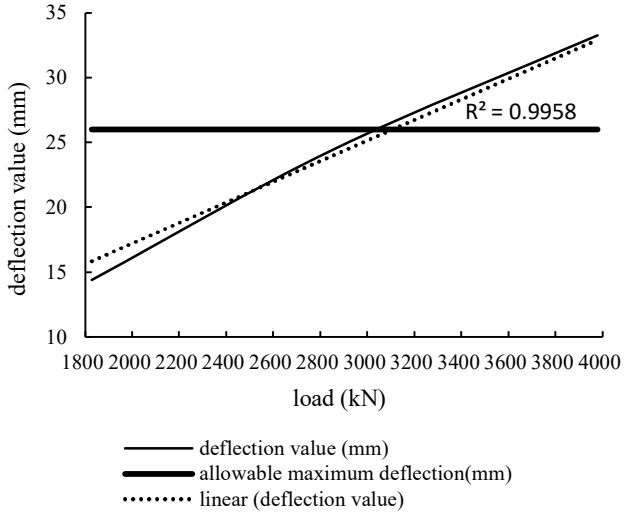

Figure 9. The relationship curve between the maximum deflection and the load value in mid-span.

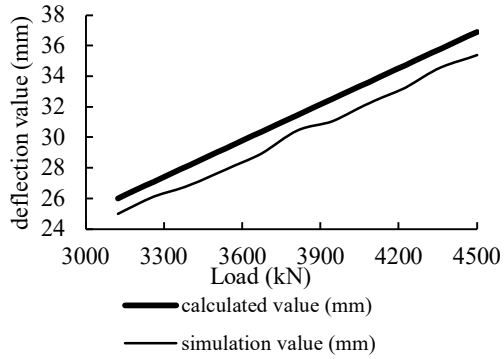

Figure 10. Data validation curve.

The trend of the relationship value is highly consistent with the simulation value of the FEM, and the relative error is controlled within 5%, which can verify that the formula is accurate and reliable.

4.3. Fatigue Safe Passage Analysis of the Taxiway Bridge Based on the Flight Growth Rate

When studying its fatigue characteristics, the annual growth rate of flights is a factor that must be considered [36]. At this stage, the load of the taxiway bridge is controlled according to the maximum landing weight [37]. According to various statistics, the average number of passing aircraft is 35 per day, so the annual take-off and landing sorties reaches 12,775, and the number of operating sorties within 20 years of service life is about 255,500. Considering that the flight growth rate of the airport is affected by economic development, region, and other factors, the annual growth rate of flights is proposed to be 3%, 5%, 7%, and 9%, respectively [1]. The operational sorties of each year in the life cycle are calculated, as shown in Table 6.

Based on the B747-400 standard operating at the maximum landing weight and 12,775 sorties per year, and considering the annual growth rates of 3%, 5%, 7%, and 9%, the change in the maximum deflection value in the mid-span after 20 years of operation of the taxiway bridge is shown in Table 7.

Table 6. Operation sorties in 1–20 years at different growth rates.

Flight Growth Rate	3%	5%	7%	9%
Year 1	12,775	12,775	12,775	12,775
Year 2	13,158	13,414	13,669	13,925
Year 3	13,553	14,084	14,626	15,178
Year 4	13,960	14,789	15,650	16,544
Year 5	14,378	15,528	16,745	18,033
Year 6	14,810	16,304	17,918	19,656
Year 7	15,254	17,120	19,172	21,425
Year 8	15,712	17,976	20,514	23,353
Year 9	16,183	18,874	21,950	25,455
Year 10	16,668	19,818	23,486	27,746
Year 11	17,169	20,809	25,130	30,243
Year 12	17,684	21,850	26,889	32,965
Year 13	18,214	22,942	28,772	35,932
Year 14	18,761	24,089	30,786	39,166
Year 15	19,323	25,294	32,941	42,691
Year16	19,903	26,558	35,247	46,533
Year 17	20,500	27,886	37,714	50,721
Year 18	21,115	29,281	40,354	55,286
Year 19	21,749	30,745	43,179	60,261
Year 20	22,401	32,282	46,201	65,685
Total sorties	343,269	422,418	523,717	653,571

Table 7. The maximum deflection of the taxiway bridge mid-span considering the annual flight growth rate.

Flight Growth Rate (%)	Maximum Deflection at the End of the 20th Year (mm)	Allowable Maximum Deflection (mm)
3	24.98	26.03
5	25.51	26.03
7	26.28	26.03
9	27.46	26.03

According to the correlation analysis, the calculation relationship is constructed as follows:

$$Y = 0.0305\alpha^2 + 0.0512\alpha + \left(Y_{max} - Y_c\right) \quad (9)$$

In the formula, Y (mm) is the maximum deflection value of the bridge deck mid-span; α is the value that removes the percentage sign of the annual growth rate of flights, i.e., 5% is recorded as $\alpha = 5$; and Y_c (mm) is the mid-span deflection caused by the weight of the taxiway bridge. The curve is shown in Figure 11, and the dotted line represents the fitting curve.

After verification, the correlation coefficient $R^2 = 0.999$, indicating that the correlation between the curve and the data is as high as 99.9%, which can be used to predict the maximum deflection value of the taxiway bridge under the fatigue state in relation to different flight growth rates, and safety redundancy analysis can be conducted [27].

It can be seen from the above figure that when the average annual growth rate of flights in that year is 6.3066%, the maximum deflection value in the middle span of the taxiway bridge reaches an allowable maximum deflection value of 26.03 mm after 20 years of operation. Therefore, the airport throughput must be strictly controlled, or the taxiway bridge must be regularly maintained, upgraded, and reconstructed to improve its bearing capacity.

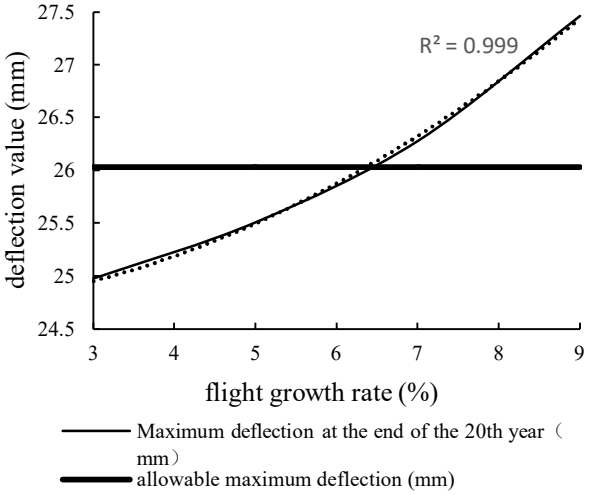

Figure 11. The maximum deflection of the taxiway bridge mid-span under different flight growth rates.

Similarly, the annual growth rate of flights continues to increase to 15% [18], the simulation value is extracted, and the relationship is verified. The following curve can be obtained as shown in Figure 12:

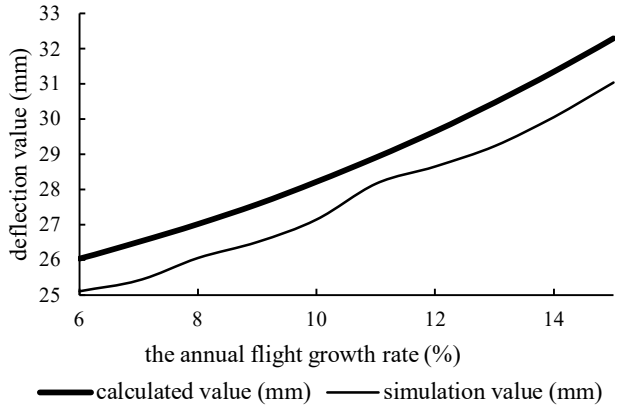

Figure 12. Data validation curve.

The curve shows that the trend of the relationship value is consistent with the simulation value, and the relative error is very small, which is controlled within 5%, indicating that the relationship is accurate and reliable, and can be used to predict the safe passage redundancy of the taxiway bridge under the fatigue state.

4.4. Prediction and Analysis of the Remaining Life of the Taxiway Bridge under the Influence of Multiple Indexes

Through the above analysis, based on the fatigue accumulation state of the taxiway bridge, the aircraft type, load, times, and the annual growth rate of flights can have an impact on the remaining traffic life of the taxiway bridge. By comprehensively considering the maximum deflection value in the middle of the existing span of the taxiway bridge, the number of passing sorties, the average annual growth rate of flights, and the single-wheel load value of the main landing gear of the aircraft, through the correlation analysis of the simulation data obtained in Sections 4.1–4.3, the relationship between the number of operations N_0 and the maximum deflection in the middle of the span, the average annual growth rate of flights, and the single-wheel load value of the main landing gear of the aircraft can be calculated as follows:

$$N_0 = 261732.8 + 10909.5Y_t - 1599.5P_t + 36728.7\alpha \quad (10)$$

N_0 is the sorties that has been operated. Y_t (mm) is the maximum deflection value of the bridge deck mid-span. α is the value that removes the percentage sign of the annual growth rate of flights. P_t (kN) is the single-wheel load value of the aircraft's main landing gear. After checking, the correlation coefficient R^2 = 0.9876, indicating that the correlation between the curve and the data is as high as 98.76%.

Several working conditions are proposed to check the accuracy of the formula, as shown below.

Working condition A: B747-400 passes through the taxiway bridge along the centerline of the bridge deck at 2857.63 kN. The maximum deflection value at the middle of the existing span is 26.28 mm, with an average annual flight growth rate of 7%.

Working condition B: B747-400 passes through the taxiway bridge along the centerline of the bridge deck at 1827.21 kN. The maximum deflection value at the middle of the existing span is 14.41 mm, with an average annual flight growth rate of 0.

Working condition C: B747-400 passes through the taxiway bridge along the centerline of the bridge deck at 2857.63 kN. The maximum deflection value at the middle of the existing span is 25.11 mm, with an average annual flight growth rate of 6%.

The data in Table 8 show that the relative error of the model is controlled within 5%, which meets the correlation requirements and can be used to deduce the remaining traffic life prediction model of the taxiway bridge under the fatigue state.

Table 8. Model validation table.

	Calculated Value/Sorties	Simulation Value/Sorties	Relative Error
Working condition A	533,569	523,717	1.85%
Working condition B	245,039	255,500	4.27%
Working condition C	484,076	469,936	2.92%

The analysis in Section 3.3 suggests that the maximum allowable deflection of the taxiway bridge is 26.03 mm. Combined with the relationship between the remaining safe passage times of the taxiway bridge under the load of the standard model obtained in Section 4.1, the calculation model of the safe passage redundancy N_s of the taxiway bridge is deduced below:

$$N_s = 261732.8 + 10909.6 \times (26.03 - Y_t) - 1599.5P_t + 36728.7\alpha \quad (11)$$

Ns (sorties) is the safe passage. *Yt* (mm) is the maximum deflection value of the bridge deck mid-span. α is the value that removes the percentage sign of the annual growth rate of flights. *Pt* (kN) is the single-wheel load value of the aircraft's main landing gear.

Combined with the conversion relationship of different types of aircraft in Section 3.1, the remaining service life of the taxiway bridge can be predicted through the following model:

$$n = \frac{\log\left(\frac{N_s \times \alpha\%}{N} + 1\right)}{\log(1 + \alpha\%)} \ (N \neq 0) \quad (12)$$

n is the remaining service life of the taxiway bridge (years). *Ns* is the safety passage (sorties). N (sorties) is the current annual traffic sorties. Y_t (mm) is the maximum deflection value of the bridge deck mid-span. α is the value that removes the percentage sign of the annual growth rate of flights. P_t (kN) is the single-wheel load value of the aircraft's main landing gear.

5. Conclusions

As taxiway bridges are important infrastructure for solving traffic conflicts in airport flight areas, the structural safety of the taxiway bridge plays a vital role in the operation efficiency of the whole airport. However, the existing taxiway bridges often run for

10–15 years without any safety detection, which presents great potential safety hazards. There is no clear index for the evaluation of its fatigue safe traffic performance. Given that the current situation struggles to detect the taxiway bridge on-site and cannot interrupt traffic, this study used a combination of theoretical analysis, experimental tests, and simulation methods to analyze its fatigue levels.

(1) The results show that the error between the extracted data of the model and the experimental data is less than 5%, which verifies the accuracy of the model and shows that the established taxiway bridge simulation model is suitable for the traffic safety analysis of the taxiway bridge.
(2) The fatigue test values of concrete and reinforcement were obtained through the test, and the S–N curve was introduced to superimpose the fatigue state of concrete and reinforcement materials into the overall structure of the bridge through the cycle.
(3) According to the data of the standard aircraft type running at the maximum landing weight in the simulation model, the mathematical relationship between the operating times and the maximum deflection in the middle of the span is derived. Combined with the load conversion method in this paper, the relationship between the operation times of any type of aircraft and the fatigue state can be studied.
(4) According to the data of 255,500 sorties of the standard aircraft type under four load levels in the simulation model, the mathematical relationship between the load of the standard model and the maximum deflection in the middle of the span was derived. t calculates that the maximum operating load under the condition of 255,500 sorties is 3130.44 kN, making it reasonably necessary to reduce the load of the aircraft.
(5) Considering the different traffic growth rates, taking the average annual 12,775 sorties as the initial value, the maximum deflection value of bridge deck was extracted when the annual growth rate of flights reaches 3%, 5%, 7%, and 9%. The mathematical relationship between the annual growth rate of departure flights and the maximum deflection value of the mid-span after 20 years was derived. It was calculated that, when the annual growth rate of flights is 6.3066%, the maximum deflection value in the life cycle of the taxiway bridge reaches the allowable maximum deflection value.
(6) According to the analysis of safe passage redundancy of the taxiway bridge under the influence of different indicators, combined with the simulation output data, the safe traffic redundancy model of the taxiway bridge under the influence of multiple indicators was obtained, and the prediction model of the fatigue residual traffic life of the taxiway bridge was deduced.
(7) The prediction model of the fatigue residual traffic life of the taxiway bridge cannot be verified by engineering measurements. Therefore, the accuracy of the model was verified according to the data output from the simulation. The accuracy of the model is more than 95% and has certain reliability. As the established taxiway bridge is based on an airport in South China, the proposed life prediction model is more suitable for this bridge and has certain limitations. In the future, more taxiway bridges should be measured, the calculation idea of remaining life should be applied to more bridge models, and the comprehensive discussion should be carried out by comparing multiple taxiway bridges to improve the models.

Author Contributions: Conceptualization, Y.Z. (Yuhui Zhang); methodology, Y.Z. (Yuhui Zhang) and Y.Z. (Yuanyuan Zhao); software, Y.Z. (Yuhui Zhang) and Y.Z. (Yuanyuan Zhao); validation, Y.Z. (Yuhui Zhang) and Y.Z. (Yuanyuan Zhao); formal analysis, Y.Z. (Yuhui Zhang); investigation, Y.Z. (Yuhui Zhang); resources, Y.Z. (Yuhui Zhang); data curation, Y.Z. (Yuanyuan Zhao); writing—original draft preparation, Y.Z. (Yuhui Zhang) and Y.Z. (Yuanyuan Zhao); writing—review and editing, Y.Z. (Yuhui Zhang) and Y.Z. (Yuanyuan Zhao); visualization, Y.Z. (Yuanyuan Zhao); supervision, Y.Z. (Yuhui Zhang); project administration, Y.Z. (Yuhui Zhang); funding acquisition, Y.Z. (Yuhui Zhang). All authors have read and agreed to the published version of the manuscript.

Funding: This research was funded by Research Funds for the Central Universities of China under grant 3122016B005.

Institutional Review Board Statement: Not applicable.

Informed Consent Statement: Not applicable.

Data Availability Statement: Data available on request.

Conflicts of Interest: The authors declare no conflict of interest.

References

1. Dong, Q.; Wang, J.H.; Zhang, X.M.; Wang, H.; Jin, X.S. Development of Virtual Load Rating Method for Taxiway Bridge under Aircraft Taxiing. *KSCE J. Civ. Eng.* **2019**, *23*, 3030–3040. [CrossRef]
2. Qi, C.X.; Zhang, X.M. Research on the Method of Fast and Accurate Taxiway Bridge Testing. *ICTIS* **2011**, 1500–1505. [CrossRef]
3. Yu, L.T.; Chen, Z.L.; Long, X.Y.; Cai, L.C.; Wang, G.H. Structural characteristics and form analysis of taxiway bridge in military airport. *IOP Conf. Ser. Earth Environ. Sci.* **2019**, *330*, 022021. [CrossRef]
4. Zhang, Y.H.; Ding, S.X. Simulation modeling of taxiway bridge under the influence of seismic wave. *Sci. Technol. Eng.* **2021**, *21*, 2518–2524.
5. Qi, C.X.; Ding, C.C.; Li, J.K. Research on optimal design of taxiway bridge based on aircraft bridge coupling vibration. *Sci. Technol. Eng.* **2022**, *22*, 6744–6751.
6. Gao, M. Research and Analysis on Mechanical Performance of Taxiway Bridge of Civil Aviation Airport. *Urban Road Bridge Flood Control.* **2021**, 93–95+15. [CrossRef]
7. Masahiro, K.; Hiroshi, S.; Kohei, S.; Kohei, Y. Behavior of steel-concrete composite deck bridge for hypothetical aircraft and regular measurement of the bridge using monitoring system. *J. Jpn. Soc. Civ. Eng. Ser. A1* **2016**, *72*, II_80–II_88. [CrossRef]
8. Zhang, X.; Yan, Y.; Dong, Q. Research on The Techniques of Dynamic Testing for Taxiway Bridge under Aircraft Taxiing. *Int. Conf. Civ. Struct. Environ. Eng.* **2016**, 257–262. [CrossRef]
9. Leitão, F.N.; da Silva, J.G.S.; Vellasco, P.D.S.; de Andrade, S.A.L.; de Lima, L.R.O. Composite (steel–concrete) highway bridge fatigue assessment. *J. Constr. Steel Res.* **2011**, *67*, 14–24. [CrossRef]
10. Bayane, I.; Mankar, A.; Brühwiler, E.; Sørensen, J.D. Quantification of traffic and temperature effects on the fatigue safety of a reinforced-concrete bridge deck based on monitoring data. *Eng. Struct.* **2019**, *196*, 109357. [CrossRef]
11. Ishida, T.; Pen, K.; Tanaka, Y.; Kashimura, K.; Iwaki, I. Numerical Simulation of Early Age Cracking of Reinforced Concrete Bridge Decks with a Full-3D Multiscale and Multi-Chemo-Physical Integrated Analysis. *Appl. Sci.* **2018**, *8*, 394. [CrossRef]
12. Lee, Y.-J.; Cho, S. SHM-Based Probabilistic Fatigue Life Prediction for Bridges Based on FE Model Updating. *Sensors* **2016**, *16*, 317. [CrossRef] [PubMed]
13. Han, Y.; Li, K.; Cai, C.S.; Wang, L.; Xu, G. Fatigue Reliability Assessment of Long-Span Steel-Truss Suspension Bridges under the Combined Action of Random Traffic and Wind Loads. *J. Bridg. Eng.* **2020**, *25*, 4020003.1–4020003.10. [CrossRef]
14. Iordachescu, M.; Valiente, A.; De Abreu, M. Fatigue life assessment of a tack welded high-strength wire mesh for reinforcement of precast concrete bridge girders. *Constr. Build. Mater.* **2018**, *197*, 421–427. [CrossRef]
15. Chen, B.; Yu, T.; Zhang, L.; Wu, Y.; Wang, Y. Research on Fatigue Performance of the Rib Beam Bridge Carriageway Slab Based on Cumulative Damage Theory. *Adv. Civ. Eng.* **2022**, *2022*, 7455038. [CrossRef]
16. Alsharari, F.; El-Zohairy, A.; Salim, H.; El-Sisi, A.E.-D. Pre-damage effect on the residual behavior of externally post-tensioned fatigued steel-concrete composite beams. *Structures* **2021**, *32*, 578–587. [CrossRef]
17. Deng, L.; Nie, L.; Zhong, W.J.; Wang, W. Developing Fatigue Vehicle Models for Bridge Fatigue Assessment under Different Traffic Conditions. *J. Bridge Eng.* **2021**, *26*. [CrossRef]
18. Saberi, M.R.; Rahai, A.R.; Sanayei, M.; Vogel, R.M. Bridge Fatigue Service-Life Estimation Using Operational Strain Measurements. *J. Bridg. Eng.* **2016**, *21*. [CrossRef]
19. Wang, H.; Qin, S.; Wang, Y. Nonlinear cumulative damage model and application to bridge fatigue life evaluation. *Adv. Struct. Eng.* **2017**, *21*, 1402–1408. [CrossRef]
20. Djoković, J.M.; Nikolić, R.R.; Bujnák, J.; Hadzima, B. Estimate of the steel bridges fatigue life by application of the fracture mechanics. *IOP Conf. Series Mater. Sci. Eng.* **2018**, *419*, 012010. [CrossRef]
21. Liu, S.Q.; Cai, S.Z.; Han, Y.; Hu, P. Stress-Level Buffeting Analysis and Wind Turbulence Intensity Effects on Fatigue Damage of Long-Span Bridges. *J. Aerosp. Eng.* **2020**, *33*. [CrossRef]
22. *JTT4-2004*; Technical Standard of Plate Rubber Bearing for Highway Bridges. Ministry of Communications of the People's Republic of China: Beijing, China, 2004.
23. *MH/T5024-2009*; Technical Specification of Civil Airport Pavement Evaluation Management. Civil Aviation Administration of China: Beijing, China, 2009.
24. Esfandiari, A.; Rahai, A.; Sanayei, M.; Bakhtiari-Nejad, F. Model updating of a concrete beam with extensive distributed damage using experimental frequency response function. *J. Bridge Eng. ASCE* **2016**, *21*. [CrossRef]
25. *JTG 3362-2018*; Code for Design of Highway Reinforced Concrete and Prestressed Concrete bridges and Culverts. China Communications Press: Beijing, China, 2018.
26. Garcia-Palencia, A.J.; Santini-Bell, E.; Sipple, J.D.; Sanayei, M. Structural model updating of an in-service bridge using dynamic data. *Struct. Control. Heal. Monit.* **2015**, *22*, 1265–1281. [CrossRef]

27. Wang, W. Fatigue consumption method for calculating the thickness of rigid pavement in civil airport. *Highw. Transp. Technol.* **2004**, 37–41.
28. Wang, W. Improvement of calculation method for remaining service life of airport pavement. *J. China Civ. Aviat. Univ.* **2004**, 37–41.
29. Deng, L.; Bi, T.; He, W.; Wang, W. Analysis Method for Load Limit Values of Reinforced Concrete Bridges Based on Fatigue Life. *J. China Highw. Eng.* **2017**, *30*, 72–78. [CrossRef]
30. Guo, M.M.; Zhang, Z.B.; Zhu, R.L. Research on fatigue performance of pre cracked concrete under tension compression cyclic load. *Sichuan Cem.* **2020**, 25.
31. Chen, P. Reliability Evaluation of Prestressed Concrete Beam Bridges under Bending Shear Stress. *Chang. Univ. Technol.* **2019**. [CrossRef]
32. Wu, R.F. Comparison and Analysis of S-N Curves in Domestic and Foreign Codes. *Ship Eng.* **2017**, *39*, 55–58+67. [CrossRef]
33. Nie, J.G.; Wang, Y.H. Comparative study on the use of the concrete constitutive model in ABAQUS to simulate the static behavior of structures. *Eng. Mech.* **2013**, *30*, 59–67+82.
34. Zhao, H.D.; Ling, J.M.; Yao, Z.K. Simplified calculation method of repeated action times of aircraft load. *J. Tongji Univ.* **2011**, *39*, 693–698.
35. Zhang, H.P.; Liu, Y.; Deng, Y.; Feng, D.M. Fatigue reliability evaluation of orthotropic plate details considering variable correlation. *Vib. Shock.* **2021**, *40*, 105–113.
36. Yuan, H.F. Design technology of Pudong airport taxiway bridge. *Urban Roads Bridges Flood Control.* **2017**, 100–101+129+13. [CrossRef]
37. Zhang, X.M.; Sun, L.L.; Hu, C.F.; Sun, Z.C. Research on Dynamic Load Coefficient Based on the Airfield Pavement Roughness. *Appl. Mech. Mater.* **2011**, *97–98*, 386–390. [CrossRef]